The EMBO Journal Vol.16 No.19 pp.5867–5879, 1997

avr-15 encodes a chloride channel subunit that mediates inhibitory glutamatergic neurotransmission and ivermectin sensitivity in *Caenorhabditis elegans*

Joseph A.Dent[1], M.Wayne Davis and Leon Avery

Department of Molecular Biology and Oncology, University of Texas Southwestern Medical Center at Dallas, 5323 Harry Hines Blvd, Dallas, TX 75235-9148, USA

[1]Corresponding author

Ivermectin is a widely used anthelmintic drug whose nematocidal mechanism is incompletely understood. We have used *Caenorhabditis elegans* as a model system to understand ivermectin's effects. We found that the M3 neurons of the *C.elegans* pharynx form fast inhibitory glutamatergic neuromuscular synapses. *avr-15*, a gene that confers ivermectin sensitivity on worms, is necessary postsynaptically for a functional M3 synapse and for the hyperpolarizing effect of glutamate on pharyngeal muscle. *avr-15* encodes two alternatively spliced channel subunits that share ligand binding and transmembrane domains and are members of the family of glutamate-gated chloride channel subunits. An *avr-15*-encoded subunit forms a homomeric channel that is ivermectin-sensitive and glutamate-gated. These results indicate that: (i) an ivermectin-sensitive chloride channel mediates fast inhibitory glutamatergic neuromuscular transmission; and (ii) a nematocidal property of ivermectin derives from its activity as an agonist of glutamate-gated chloride channels in essential excitable cells such as those of the pharynx.

Keywords: avermectins/*Caenorhabditis elegans*/channel/glutamate/helminth

Introduction

Ivermectin is a potent anthelmintic drug that is widely used to treat nematode infections in livestock (Campbell, 1989) but is also the drug of choice in the treatment of onchocerciasis (river blindness) (Liu and Weller, 1996). The target of ivermectin is supposed to be glutamate-gated chloride channels. Ivermectin increases chloride permeability in insect neurons (Lees and Beadle, 1986) and muscles (Duce and Scott, 1985) as well as in crustacean muscle (Fritz *et al.*, 1979; Mellin *et al.*, 1983). Ivermectin opens chloride channels in outside-out patches from *Ascaris suum* (nematode) muscle membrane (Martin and Pennington, 1989). When applied to outside-out patches of crayfish muscle, ivermectin and glutamate appear to increase the open time of the same chloride channel (Zufall *et al.*, 1989). A cDNA has been cloned from *Caenorhabditis elegans* which encodes a protein, GluClα, that forms homomeric ivermectin-sensitive chloride channels when expressed in *Xenopus* oocytes (Cully *et al.*, 1994). In addition, this ivermectin-sensitive channel can associate with a glutamate-gated channel subunit from *C.elegans*, GluClβ, to form a channel that is both ivermectin-sensitive and glutamate-gated (Cully *et al.*, 1994).

However, there is no direct evidence linking GluClα to the *in vivo* effects of ivermectin on worms. Although GluClα has been proposed to mediate neurotransmission at inhibitory glutamatergic synapses, GluClα must associate with GluClβ in order to respond to glutamate (Cully *et al.*, 1994). There is no evidence that these subunits associate or are even co-expressed in the organism and no inhibitory glutamatergic synapses have been characterized in nematodes (Geary *et al.*, 1992). Determining the role of GluClα is complicated further by indications that avermectins potentiate gating of GABA-gated channels by GABA (Pong and Wang, 1982; Sigel and Baur, 1987) or reduce the mean channel current (Martin and Pennington, 1989). Since GABA-gated channels are expressed in nematodes (see Martin, 1993; McIntire *et al.*, 1993a,b) they are also potentially relevant targets of avermectins.

Caenorhabditis elegans is a useful system in which to understand the mechanism of ivermectin's action in nematodes. Ivermectin prevents growth of *C.elegans* at a concentration of <10 ng/ml (J.Dent, unpublished observation) and induces paralysis at ~20 ng/ml (Arena *et al.*, 1995). One obvious effect of ivermectin on *C.elegans* and other nematodes is that it inhibits pharyngeal pumping (Bottjer and Bone, 1985; Avery and Horvitz, 1990; Geary *et al.*, 1993). In order for *C.elegans* to eat, the pharynx, a neuromuscular organ, must pump rhythmically with a cycle of contraction and relaxation. The pharynx forms a tube made up of 20 muscle cells of eight anatomical types and 20 neurons of 14 anatomical types (see Figure 6A; Albertson and Thomson, 1976). Contraction of the radially oriented pharyngeal myofibrils pulls the walls of the anterior (corpus) pharyngeal lumen apart, opening the pharynx. Liquid and the suspended bacterial food are thereby sucked into the worm. Muscle relaxation results in the rapid collapse of the walls of the lumen, forcing liquid out of the anterior pharynx while trapping the suspended bacteria. Peristalsis of the isthmus transports bacteria to the terminal bulb where they are ground to a digestible pulp and deposited in the intestine.

The timing of pharyngeal muscle relaxation is important for proper trapping of bacteria (Avery, 1993a). A bilaterally symmetric pair of pharyngeal motor neurons, the M3s, which synapse on the corpus muscle (Albertson and Thomson, 1976; see Figure 6A), modulate the timing of relaxation. The M3s generate inhibitory postsynaptic potentials (IPSPs) in the contracted pharyngeal muscle. When the M3 neurons are ablated with a laser, the IPSPs disappear and the muscle contractions have a longer average duration (Avery, 1993b; Raizen and Avery, 1994). Although GABAergic neurotransmission exists in

C.elegans (McIntire *et al.*, 1993a,b), the M3 neurons are clearly not GABAergic since they do not stain with antibodies to GABA (McIntire *et al.*, 1993b) and mutants that lack GABAergic neurotransmission retain M3-generated IPSPs (Raizen and Avery, 1994).

Since ivermectin inhibits pharyngeal pumping in *C.elegans* and the nematode expresses ivermectin- and glutamate-sensitive channels, we hypothesized that the inhibitory postsynaptic potentials generated by the M3 motor neuron might be the result of fast inhibitory glutamatergic neurotransmission mediated by an ivermectin-sensitive chloride channel. We confirmed our hypothesis by showing that: (i) the pharynx responds to iontophoretically applied glutamate by hyperpolarizing; (ii) the response to glutamate is absent in *avr-15*, a mutant that lacks M3 IPSPs and that confers synthetic ivermectin resistance on worms; and (iii) *avr-15* codes for a protein that is a member of the family of ivermectin-sensitive and glutamate-gated chloride channel subunits. These results demonstrate the role of glutamate-gated channels in the nematocidal mechanism of ivermectin and identify the pharynx as an essential organ that is targeted by ivermectin. The results also suggest that the presence of multiple ivermectin targets may explain the absence of widespread ivermectin resistance.

Results

Iontophoretic application of glutamate to pharyngeal muscle mimics the effects of M3 activity

If the M3 neurons are glutamatergic, then iontophoretic application of glutamate directly to the pharyngeal muscle should mimic the ability of the M3 neurons to hyperpolarize the muscle and shorten the duration of muscle contraction during a pump. To test this, we used an exposed pharynx preparation. To expose the pharynx, the worm was bisected at the pharyngeo-intestinal valve. The remaining cuticle surrounding the pharynx was retracted, exposing the terminal bulb and the posterior corpus muscles which are innervated by the M3 neurons. In the proper saline solution, the pharynx continues to pump normally and produces a normal electropharyngeogram (EPG) (Davis *et al.*, 1995). Application of glutamate iontophoretically to corpus muscle beginning immediately after the initiation of a pump substantially shortened the pump duration (Figure 1A and B). Thus, glutamate hastens hyperpolarization of contracted, depolarized pharyngeal muscle. Since photolytic release of caged glutamate onto the pharyngeal muscle during a pump produced IPSP-like spikes in an EPG (H.Li, W.Denk, L.Avery and G.Hess, unpublished observation), presumably iontophoresed glutamate is also producing IPSPs, but these are so large that they prematurely return the pharyngeal muscle to the resting potential. Iontophoretic application of aspartate had no effect on pump duration, ruling out the possibility that decreased pump duration is an electrical stimulus artifact (Figure 1B). In a blind comparison of six aspartate samples and six glutamate samples, we were able to identify the glutamate samples by their effect on pump duration ($P < 0.005$).

To exclude the possibility that the glutamate acted on the muscle indirectly by stimulating the M3 neurons, we ablated the M3 neurons with a laser. In their absence, the muscle still responded to glutamate (Figure 1B). To determine whether a chloride channel mediated the effect of glutamate on the pharyngeal muscle, we altered the external chloride concentration. If the effect of glutamate on the pharyngeal muscle is mediated by a chloride channel, then a sufficient reduction in the external chloride concentration should cause glutamate to depolarize the muscle. When the chloride concentration was reduced from 153 mM to 14 mM, glutamate extended pump duration; raising the chloride concentration restored the ability of glutamate to shorten pump duration (Figure 1C).

avr-15 is necessary for M3 activity and confers ivermectin sensitivity

In the course of a screen for starved mutants that have abnormal EPGs, we found one, *ad1051*, that lacked M3 IPSPs (Figure 2A) and was slightly starved but otherwise appeared normal. We showed that *ad1051* mapped under the deficiency *nDf42* on chromosome V and that *ad1051* did not complement *avr-15(nr395)*, indicating that *ad1051* is an allele of *avr-15*. Furthermore, the phenotype of *avr-15(ad1051)/nDf42* was not obviously worse than that of the *avr-15(ad1051)* homozygote, consistent with the possibility that *ad1051* is a null allele.

Alleles of *avr-15* were first identified because they confer recessive synthetic resistance to ivermectin in combination with mutations in other *avr* genes (Rand and Johnson, 1995; C.D.Johnson, unpublished observation cited in Anderson, 1995). Single mutant strains homozygous for *avr-15* mutations (including *ad1051*) display little or no resistance. To determine whether *avr-15(ad1051)* can confer synthetic resistance, we selected for mutants in an *avr-15(ad1051)* background that were resistant to 10 ng/ml ivermectin. Mutants were identified at a rate of $>$1:1700 per haploid genome, which is consistent with the frequency for loss-of-function alleles. The resistance genes from one resistant strain were mapped. Mutations in two genes were necessary for resistance, *avr-15(ad1051)* and a gene on chromosome I [*avr(ad1302)*]. Thus, *avr-15(ad1051)* confers synthetic resistance to ivermectin in conjunction with at least one other gene.

avr-15 is necessary for the pharyngeal muscle to respond to iontophoretically applied glutamate

Since *avr-15* confers sensitivity to ivermectin and ivermectin is thought to be an agonist of glutamate-gated chloride channels, one possibility was that *avr-15* encodes a subunit of an ivermectin-sensitive glutamate-gated channel. If *avr-15* encodes a glutamate receptor subunit present in the postsynaptic muscle membrane, then pharynxes from *avr-15* mutants should not respond to iontophoretically applied glutamate. As a control in these experiments, we used a previously identified mutant, *eat-4*, that also lacks M3 activity but is thought to act presynaptically (R.Y.N.Lee, personal communication). In a blind comparison, we were able to identify the genotypes of six *avr-15(ad1051)* and six *eat-4(ad572)* worms because the pharynxes of *avr-15* mutants did not respond to glutamate, whereas the pharynxes from *eat-4* mutants did ($P < 0.005$; Figure 2B). Thus, *avr-15* acts postsynaptically in the pharyngeal

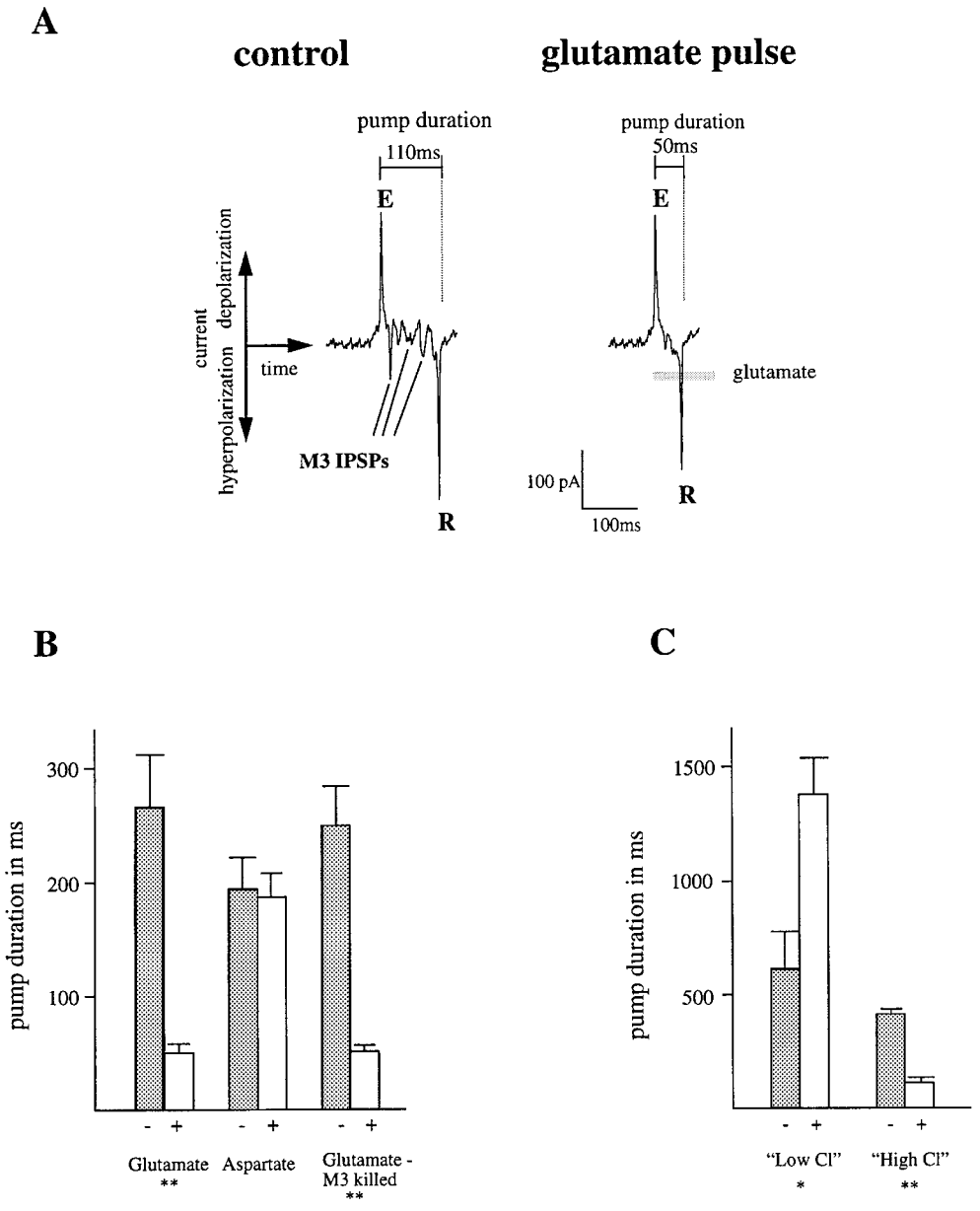

Fig. 1. Effects of iontophoresis of glutamate on pharyngeal pump duration. (**A**) Electropharyngeogram (EPG) of a wild-type exposed pharynx and of a wild-type pharynx to which glutamate was applied iontophoretically during the 100 ms period indicated by the bar. The EPG corresponds approximately to the time derivative of the pharyngeal muscle membrane potential (Raizen and Avery, 1994). The first upward spike (E) marks the depolarization of the muscle membrane that initiates muscle contraction. The large downward spike (R) marks the repolarization of the corpus muscle that precedes corpus muscle relaxation. During the period of depolarization, inhibitory postsynaptic potentials (IPSPs) from the M3 motor neurons are evident. The iontophoretic application of glutamate shortens the duration of the action potential to 50 ms. (**B**) Effect of glutamate and aspartate on average pump duration in exposed wild-type pharynxes and in exposed pharynxes lacking M3 neurons. Ten pumps were measured from each pharynx; five pumps with no delay between the E spike and application of glutamate or aspartate (+), alternating with five pumps during which the application of glutamate or aspartate was delayed until 400 ms after the E spike (–). The duration of the pump was determined by the time between the E and R spikes. Error bars indicate 1 SEM. (**C**) The effect of glutamate in low-chloride solution. Each wild-type pharynx was tested for the ability of glutamate to shorten the pump duration in 14 mM ('low') chloride solution and retested after raising the chloride concentration to 84 mM ('high'). '**' and '*' indicate that the difference between the + and – bars is statistically significant at $P < 0.005$ and $P < 0.01$ respectively.

muscle whereas *eat-4* acts presynaptically, presumably in the M3 neuron itself.

Alternatively spliced chloride channel subunits map near avr-15

Our results indicated that *avr-15* might encode a glutamate- and ivermectin-sensitive chloride channel subunit. To test this idea, we used PCR to generate a 2.2 kb GluClα (Cully *et al.*, 1994) genomic DNA clone that was used to probe a YAC grid. The GluClα probe hybridized strongly to three overlapping YACs (Y55D7, Y56A6 and Y42B4; Figure 3A). These YACs presumably represent the map position of GluClα, which is not consistent with the map position of *avr-15*. In addition, the GluClα probe hybridized weakly to three overlapping YACs (Y47E2, Y55E8 and Y53F11; Figure 3A) that map under *nDf42*,

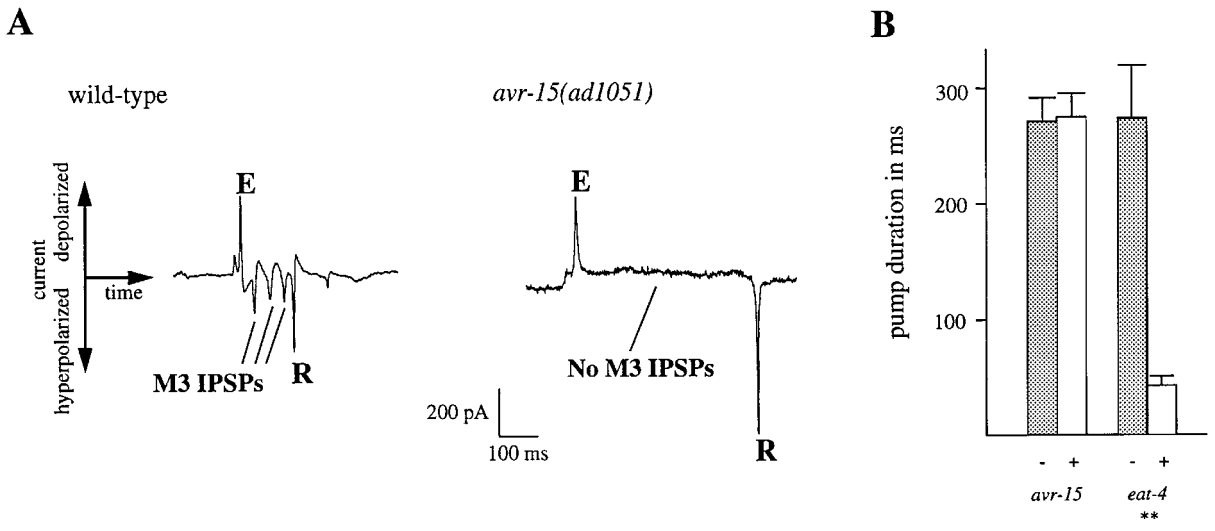

Fig. 2. (**A**) Electropharyngeogram of whole wild-type and *avr-15(ad1051)* mutant worms. Interpretation of the trace is as described in Figure 1. (**B**) The effect of iontophoretically applied glutamate on the average pump duration of dissected pharynxes from *eat-4(ad572)* and *avr-15(ad1051)* mutants. (+) indicates glutamate was applied immediately after the E spike; (–) indicates the glutamate pulse was delayed 400 ms after the E spike. Error bars indicate SEM. '**' indicates that the difference between the + and – bars is statistically significant at $P < 0.005$.

consistent with the map position of *avr-15*. The region where these YACs overlap is covered by the cosmid K10B8 (Figure 3B). We used GluClα to probe Southern blots of K10B8 restriction digests; the regions of K10B8 identified by the GluClα probe were sequenced and found to encode open reading frames with significant similarity to GluClα. Two alternatively spliced cDNAs of 2.2 kb and 1.7 kb were identified that correspond to chloride channel subunits encoded by the GluClα-like gene on K10B8. Bands whose sizes corresponded to that of the two cDNAs were identified on a Northern blot. The 1.7 kb cDNA appeared to be expressed at a level at least twice that of the 2.2 kb cDNA (Figure 4).

GluClα2 belongs to the family of ivermectin-sensitive glutamate-gated chloride channel subunits

The transcripts encoded by K10B8 contain open reading frames that predict mature proteins of 459 amino acids (mol. wt ~53 kDa) and 630 amino acids (mol. wt ~72 kDa; Figure 5). When compared with a protein database, the highest degree of similarity is to GluClα, followed by GluClβ, the *Drosophila* glutamate-gated chloride channel and then the mammalian glycine-gated channel subunits (α and β). Between amino acids 45 and 379—the extracellular ligand-binding domain through the third transmembrane domain, a region characterized by few homology gaps—the putative open reading frame has 83% amino acid identity to GluClα but only 54% identity to GluClβ and 53% identity to the *Drosophila* glutamate-gated channel (Figure 5). The alternatively spliced transcripts share the exons encoding the putative transmembrane and ligand binding domains which are the regions of the channel subunits that are homologous to other ligand-gated channel subunits. The non-shared domains, which are part of the putative extracellular domain, consist of 23 amino acids (1.7 kb transcript) and 202 amino acids (2.2 kb transcript) and have no significant similarity to anything in the database. The predicted proteins from both transcripts begin with consensus signal peptides that are predicted to be cleaved at amino acids 23 (1.7 kb) and 27 (2.2 kb; von Heijne, 1986). Since the homology to GluClα is comparable with the level of homology among sequences within a subclass of $GABA_A$ or glycine channel subunits (70–80%; Grenningloh *et al.*, 1990; Bechade *et al.*, 1994; Macdonald and Olsen, 1994) whereas the homology to GluClβ is comparable with the homology among $GABA_A$ or glycine channel subclasses, the chloride channel subunits encoded by K10B8 and GluClα appear to define a subclass of the ivermectin-sensitive chloride channel subunits. Hence, we will refer to the channel subunits encoded by the K10B8 as GluClα2A (2.2 kb) and GluClα2B (1.7 kb) and the original GluClα subunit as GluClα1.

GluClα2A and B have features typical of ligand-gated chloride channels (Figure 5). The four putative transmembrane domains are the most conserved regions within this family of proteins (see also Cully *et al.*, 1994 for a characterization of regions of homology between the glutamate-gated channel subunits and other ligand-gated chloride channels). GluClα2A contains three predicted extracellular N-linked glycosylation sites, one of which, N397, is conserved on both GluClα1 and GluClβ. There is a predicted phosphorylation site in the intracellular domain between transmembrane regions three and four, T524, that is conserved in GluClα1. Cysteines in the extracellular domain that are conserved in glycine- and GABA-gated channels are also present in GluClα2. An unusual feature of GluClα2A is its large, ~420 amino acid extracellular domain characterized by a 35 residue-long acidic stretch that contains 21 aspartate or glutamate residues (Figure 5).

avr-15 encodes GluClα2

Based on the electrophysiological results, we predicted that *avr-15* would be expressed in the pharyngeal muscles onto which M3 synapses. A 6 kb DNA fragment that encodes the first three exons of GluClα2A fused to green fluorescent protein (GFP) was used to transform worms. The transformed animals exhibited fluorescence in all of

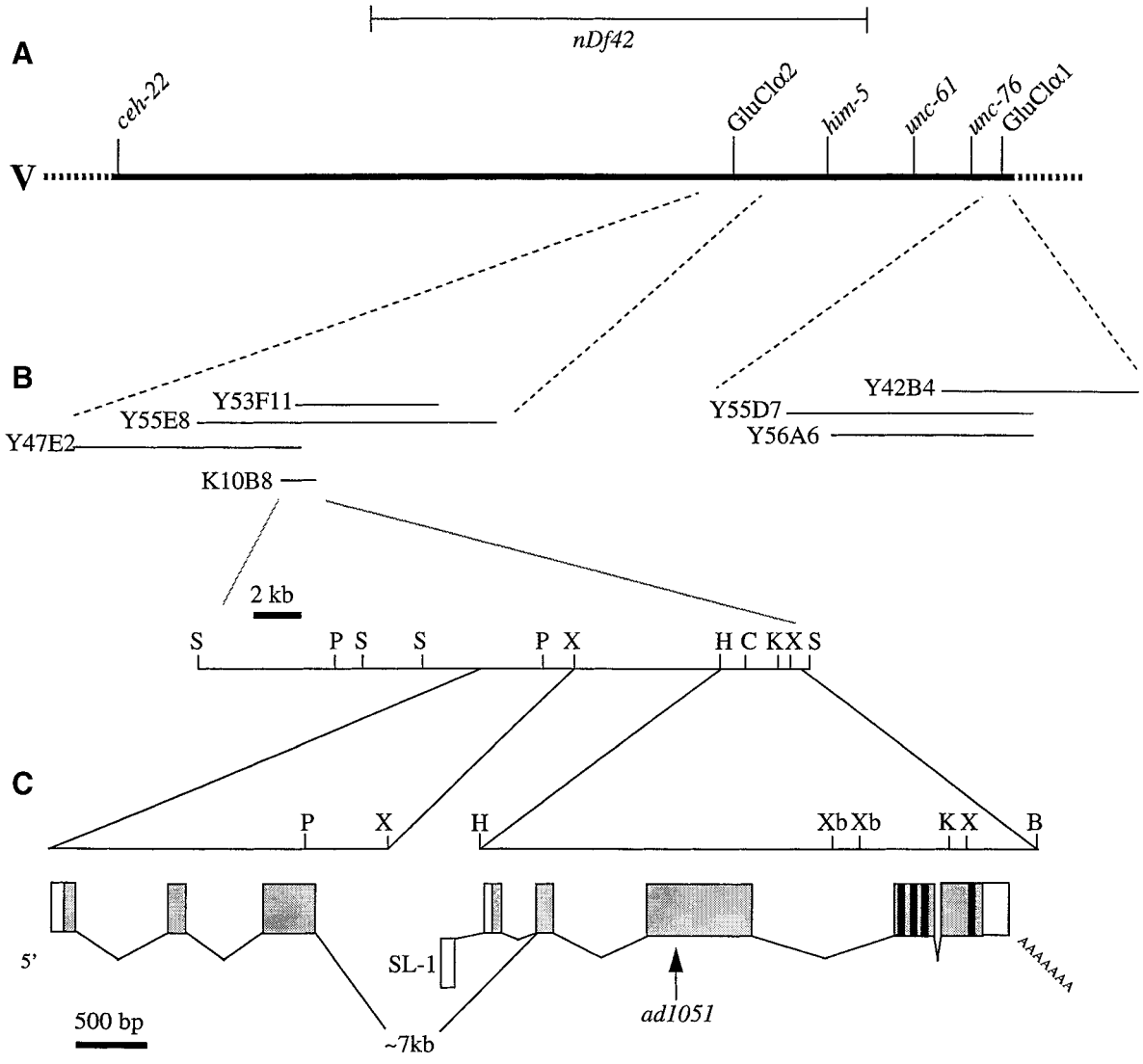

Fig. 3. Genetic and physical map in the region of *avr-15*. (**A**) The genetic map in the region of *avr-15*. *avr-15* lies under *nDf42* which lies between *ceh-22* and *unc-76*. (**B**) The physical map. The strongly hybridizing signal that appears when a YAC grid is probed with GluClα1 maps to YACs that lie to the right of *unc-76* and is therefore not consistent with GluClα1 being encoded by *avr-15*. The weakly hybridizing YACs (indicated as GluClα2) map between *ceh-22* and *him-5* and are therefore consistent with the map position of *avr-15*. (**C**) Map of the cosmid K10B8. Exons 4 and 5 are separated by an ~8 kb intron. *ad1051* indicates the position of the *avr-15(ad1051)* nonsense mutation. Restriction sites: S, *Sac*I; X, *Xho*I; K, *Kpn*I; P, *Pst*I; Xb, *Xba*I; B, *Bam*HI. The orientation of the restriction map of K10B8 is shown inverted relative to the genetic map.

the muscles of the metacorpus (pm4) and the isthmus (pm5), precisely those muscles onto which M3 synapses (Albertson and Thomson, 1976; Figure 6A and B). The GFP staining of pharyngeal muscle began shortly before hatching and persisted throughout adulthood. Strong staining was also seen in a few neurons of the head, including RMED, RMEV and the bilaterally symmetric RMGs (data not shown). Weak staining was seen in unidentified ventrally located neurons contributing to the dorsal and ventral sublateral nerve cords. Two ventral cord neurons near the anus stain consistently, namely DA9 and a more anteriorly located neuron that is likely to be VA12. Thus, the GluClα2A promoter is active in pharyngeal muscle as well as some motor neurons, suggesting that GluClα2A is also expressed in these cells.

If *avr-15* encodes GluClα2A or B, then *avr-15(ad1051)* would be expected to contain a disabling mutation in the chloride channel open reading frame. The GluClα2 gene from *avr-15(ad1051)* worms was sequenced and found to contain a G→A transition in the third position of the W271 codon (of GluClα2A) which creates an opal stop codon. Because the *ad1051* nonsense mutation occurs relatively early in the gene, before the four transmembrane domains, and since it is in an exon that is shared by both transcripts, *ad1051* is likely to be a null allele of both gene products. A Northern blot of *avr-15(ad1051)* worms shows that the levels of both transcripts are reduced at least 2-fold and 4-fold for GluClα2A and GluClα2B respectively (Figure 4). There is a system in *C.elegans* which degrades RNAs that contain nonsense mutations and which would account for the reduction in the levels of the GluClα2A and GluClα2B transcripts (Pulak and Anderson, 1993).

When used to stably transform *avr-15(ad1051)* worms, the cosmid K10B8 restores M3 IPSPs to the pharyngeal muscle (data not shown). To confirm that GluClα2 is the

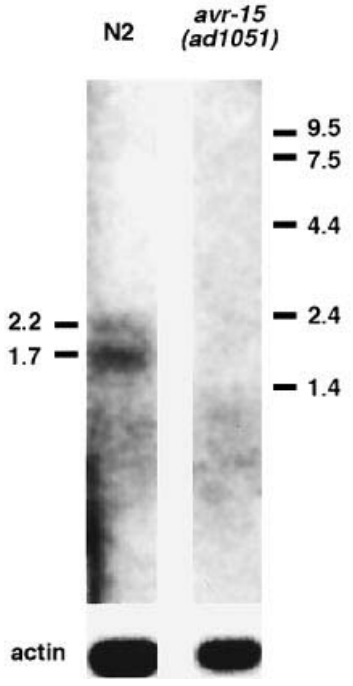

Fig. 4. Northern blot of wild-type and *avr-15(ad1051)* strains. Poly(A)$^+$ selected RNA was probed with 773 bp of DNA corresponding to the 5′ end of GluClα2A including 171 bp that overlap both GluClα2A and GluClα2B. Numbers to the left mark the position of the molecular weight standards and numbers to the right indicate the estimated molecular weight of the two bands detected in the wild-type. No bands were evident in the *avr-15(ad1051)* lane. The bands at the bottom are the same blot probed with an actin probe which acts as a loading control.

relevant transcript from K10B8, we generated a construct that places the GluClα2A cDNA under the transcriptional control of the *myo-2* promoter. The *myo-2* promoter specifically drives expression in a subset of pharyngeal muscles including pm4, the muscle onto which M3 synapses (Okkema *et al.*, 1993). When stably transformed into the ivermectin-resistant strain DA1302 [*avr(ad1302)* I; *avr-15(ad1051)* V], the *myo-2*::GluClα2A construct also restores M3 IPSPs to the pharyngeal muscle (data not shown).

Finally, to determine whether GluClα2 also rescues the ivermectin resistance phenotype, we tested the ivermectin resistance of the *avr(ad1302)* I; *avr-15(ad1051)* V; *myo-2*::GluClα2A strain. Since, in the *myo-2*::GluClα2A-carrying strain, the extrachromosomal arrays formed by exogenous DNA are only transmitted to ~20% of the progeny of transformed worms, we tested mixed populations of transformed and non-transformed worms for sensitivity to ivermectin. When a mixed population of worms was grown on 10 ng/ml ivermectin, none of the adult worms expressed the roller phenotype of the dominant *rol-6* co-transformation marker, indicating that worms carrying *myo-2*::GluClα2A had become ivermectin-sensitive and were arrested as larvae (data not shown).

GluClα2A forms a homomeric ivermectin-sensitive and glutamate-gated channel

In order to clarify the role of the GluClα2A subunit in glutamate-gating and ivermectin sensitivity, we expressed the subunit in *Xenopus* oocytes. Either RNA transcribed from the GluClα2A open reading frame or water was injected into oocytes and allowed to express. RNA-injected but not water-injected oocytes exhibited reversible, glutamate-gated currents that desensitized rapidly in a concentration-dependent manner (Figure 7A). The channels responded to as little as 100 μM glutamate but did not respond to 1 mM glycine or 1 mM GABA (data not shown). Maximal responses to glutamate at 10 mM were obtained 30 s after the glutamate had been washed out, indicating the recovery from desensitization was also rapid. A concentration–response curve indicated an EC_{50} of 2.0 ± 0.3 mM glutamate with an estimated Hill coefficient of 1.5 (Figure 7A; see Materials and methods for an explanation of calculations).

When ivermectin was applied at a concentration of 10 μM, a slowly desensitizing current was generated which was not reversed when the bath solution was replaced by Ringers (Figure 7B). The maximal ivermectin-induced current was on average 30 (±6)-fold greater (n = 4) than the maximal current obtained from previous exposure of the same oocyte to 10 mM glutamate. At a concentration of 0.5 mM, ibotenate produced a response that was 6 ± 2% of the maximal response from 10 mM glutamate (n = 6). The GluClα2B cDNA encodes a channel that responds to both glutamate and ivermectin with similar kinetics to those exhibited by GluClα2A (data not shown).

An *I–V* curve of the GluClα2A channel after exposure to 10 μM ivermectin is shown in Figure 7C. In Ringers, the current is outwardly rectifying and the average reversal potential is –20 ± 3 mV (n = 5), consistent with a calculated Nernst potential for chloride of –19 mV assuming 50 mM internal chloride (Kusano *et al.*, 1982). When the sodium chloride in the Ringers was replaced by sodium gluconate, the reversal potential shifted positively to over +30 mV (calculated reversal potential for 8 mM external chloride is +46 mV). Thus, GluClα2 forms a glutamate- and ivermectin-sensitive chloride channel.

Discussion

AVR-15/GluClα2 is a member of the family of glutamate-gated chloride channel subunits

The family of glutamate-gated chloride channel subunits has many parallels to the other ligand-gated chloride channels. The fact that GluClα2 shares such a high level of identity with GluClα1, comparable with the homology shared by $GABA_A$ or glycine receptor subunits within a single class (α or β for glycine channels, Bechade *et al.*, 1994; α, β, γ, δ or ρ for $GABA_A$ channels, Macdonald and Olsen, 1994), suggests that the family of glutamate-gated chloride channel subunits is similarly diverse and that further members of the α and/or β classes as well as new classes of subunits may remain to be identified. A cursory examination of the *C.elegans* genome that has been sequenced so far (~70% of the genome) indicates the presence of a multitude of potential chloride channel genes (J.Dent, unpublished observation). The fact that ivermectin resistance is synthetic suggests the possibility that loss-of-function mutations in a gene(s) encoding other ivermectin-sensitive channel subunits may confer, in combination with *avr-15*, high-level ivermectin resistance. Since *avr(ad1302)* maps to chromosome I and GluClα1

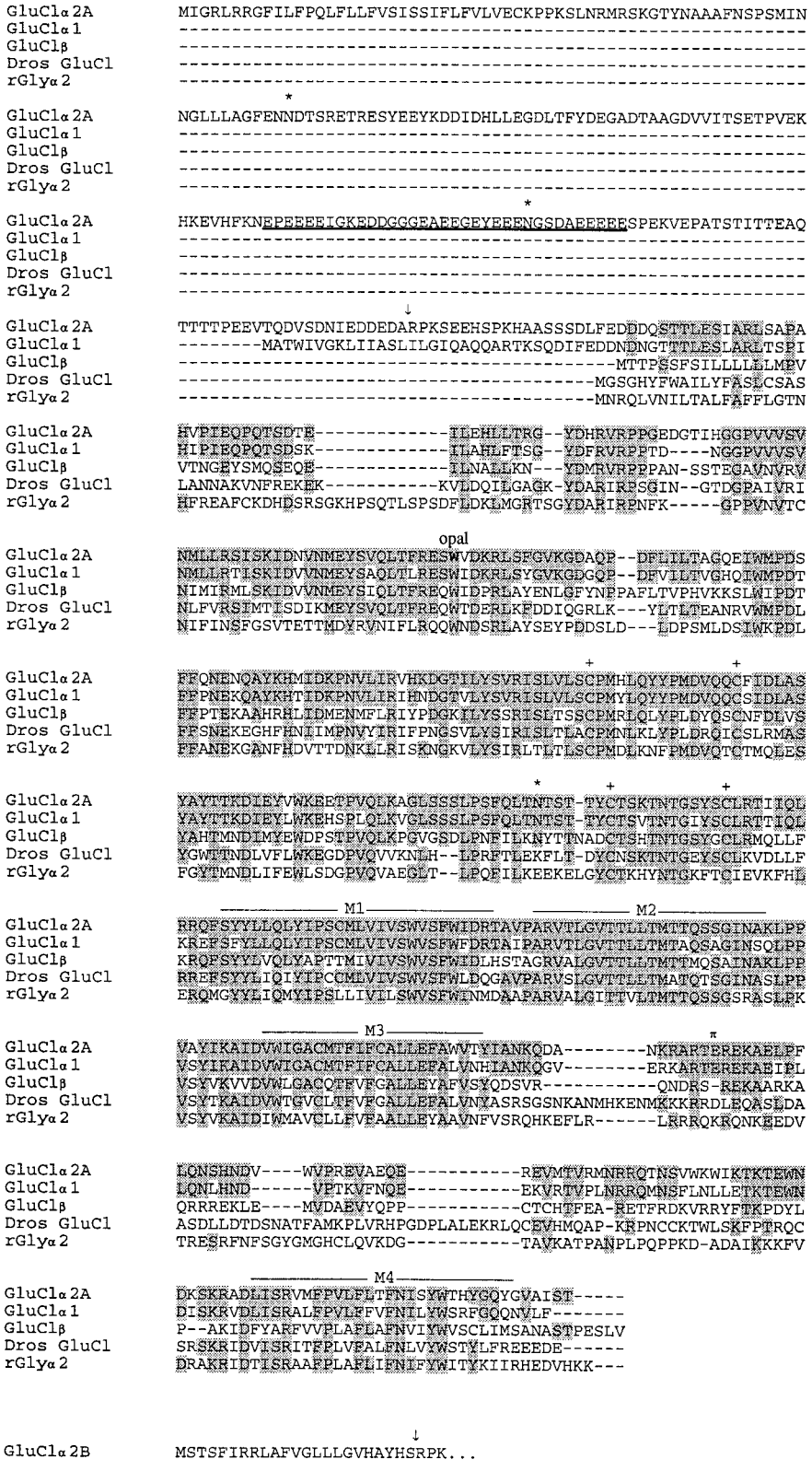

Fig. 5. Alignment of GluClα2 with other ligand-gated chloride channels subunits. The shaded amino acids are identical to GluClα2A. The bold W indicates the position of the opal nonsense mutation in *ad1051*. The '*' indicates putative N-linked glycosylation sites. The '+' indicates cysteine residues in the extracellular domain that are conserved among glutamate- or glycine-gated chloride channels. 'π' indicates a potential PKA and PKC phosphorylation site conserved between GluClα2 and GluClα1. The acidic region of the putative extracellular domain is underlined. GluClα1 and GluClβ are *C.elegans* ivermectin- and glutamate-gated channel subunits (Cully *et al.*, 1994); Dros GluCl is a *Drosophila melanogaster* ivermectin- and glutamate-gated subunit (Cully *et al.*, 1996); rGlyα2 is a rat glycine channel subunit, (Kuhse *et al.*, 1991). The sequence of the alternatively spliced amino-terminal domain present in GluClα2B is shown at the bottom. The arrows indicate the points at which the amino acids sequences of the two proteins converge. Sequences were aligned using CLUSTAL W (Thompson *et al.*, 1994) and annotated using DNA DRAW.

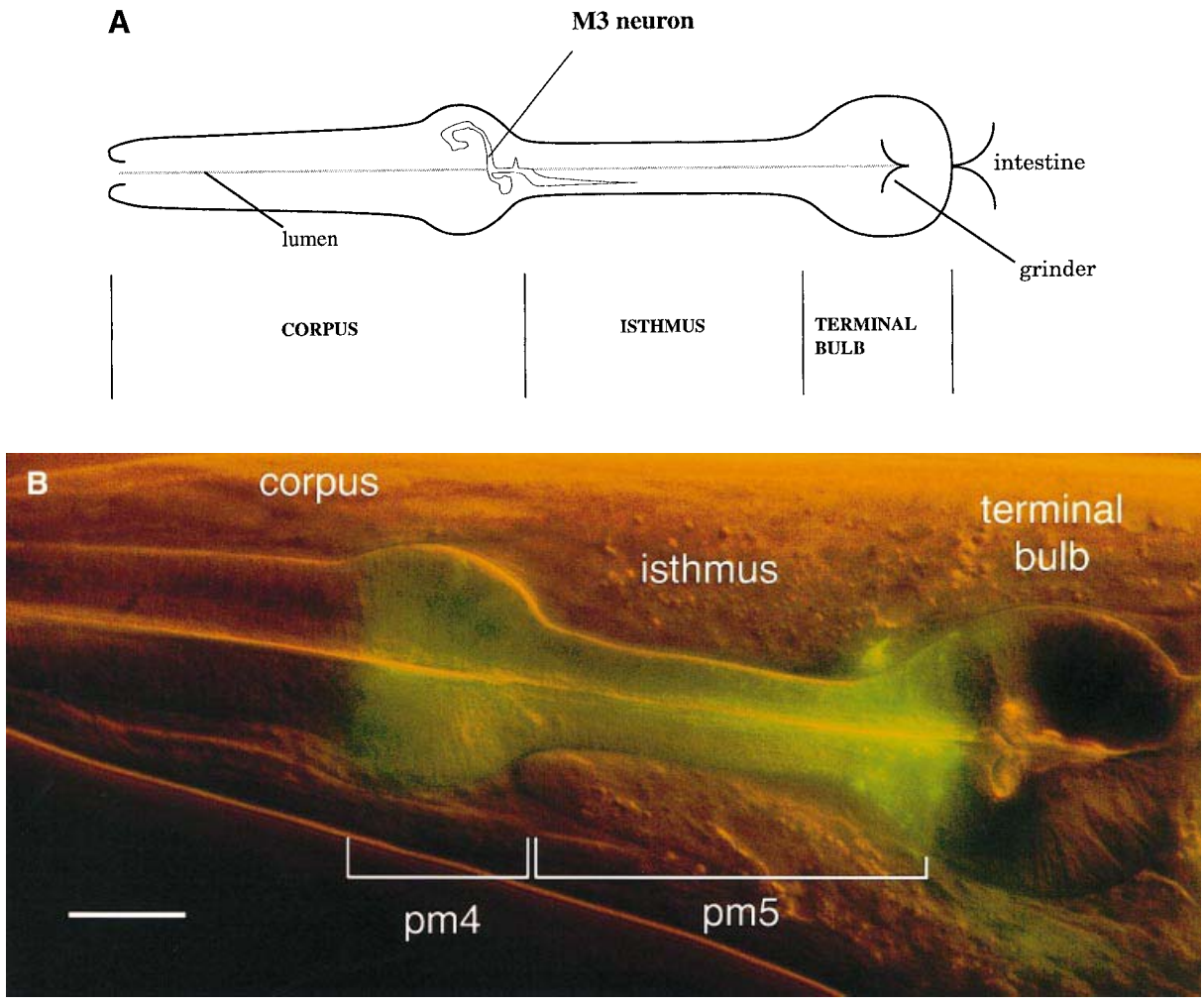

Fig. 6. Pharyngeal anatomy and expression pattern of a GluClα2A::GFP promoter fusion. (**A**) A side view of the pharynx (anterior is to the left) showing where one of the bilaterally paired M3 motor neurons is located. The neurons are embedded in folds in basal membranes of the 3-fold symmetric pharyngeal muscles and form synapses primarily onto the pm4 pharyngeal muscles, which form the metacorpus (the posterior bulb of the corpus). The pharynx of an adult worm is ~200 μm in length. (**B**) Fluorescence staining in the pharynx of a worm transformed with a GluClα2A::GFP promoter fusion construct. Anterior is left and ventral is down. The fluorescence is limited to the pharyngeal muscles pm4 and pm5 as indicated in the diagram. The out-of-focus extrapharyngeal staining is in neurons. The scale bar (lower left) indicates 20 μm.

is on chromosome V, there may be a third GluClα subunit encoded by *avr(ad1302)*.

Presumably, as for the other ligand-gated channels (Macdonald and Olsen, 1994), the subunits from different classes of the GluCl family assemble into a pentameric channel. The stoichiometry for GABA- and glycine-gated channels is thought to be (2α)(2β)(γ) and (3α)(2β) respectively (Bechade *et al.*, 1994; Chang *et al.*, 1996). It has been shown that GluClα1 and GluClβ can associate to form channels in *Xenopus* oocytes (Cully *et al.*, 1994). Since GluClα2 forms a homomeric channel that responds to both glutamate and ivermectin, it could in principle act as a homomer to mediate M3 neurotransmission. However, we think this is unlikely because: (i) GluClα2A is relatively unresponsive to glutamate (EC_{50} = 2 mM) compared with GluClβ (EC_{50} = 380 μM; Cully *et al.*, 1994) and the *Drosophila* glutamate-gated channel (EC_{50} = 23 μM; Cully *et al.*, 1996); and (ii) we found that the patterns of expression of the GluClα2A and GluClβ promoters overlap in the pharyngeal muscle pm4, suggesting that the two subunits associate to form the M3 receptor (Laughton *et al.*, 1995). The fact that mutations in *avr-15* result in the absence of M3 neurotransmission and the absence of a pharyngeal response to glutamate indicates that, if there are other subunits of the M3 receptor, such as GluClβ, they cannot form a functional channel without GluClα2.

GluClα2A combines properties seen in other glutamate-gated chloride channel subunits: (i) it responds to both glutamate and ivermectin; (ii) the ivermectin-induced response partially densensitizes; and (iii) the glutamate response desensitizes rapidly. Etter *et al.* (1996) showed that a single amino acid change (T308A or G) in the M2 transmembrane domain of GluClα1 generated a channel subunit that exhibited behaviors very similar to those exhibited by GluClα2A. The GluCl channel from *Drosophila* also responds to both ligands and has a rapidly desensitizing glutamate current (Cully *et al.*, 1996). Thus, small changes in channel structure can affect the linkage of ligand binding to channel gating as well as the kinetics of desensitization. Interestingly, T308 is conserved between GluClα2 and GluClα1.

Like some subunits of the $GABA_A$ and glycine receptor families, GluClα2 is alternatively spliced. Splice variants of mammalian GABA γ2 and glycine α1 channel subunits

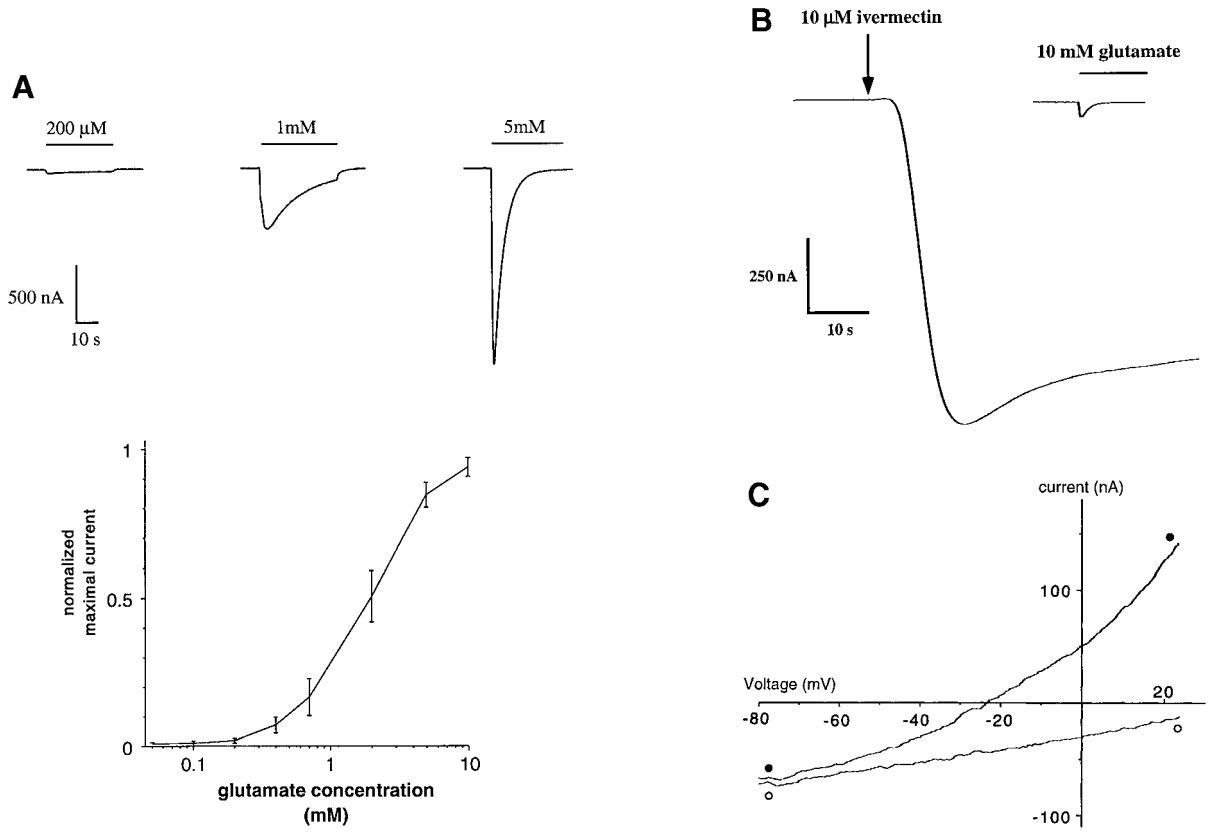

Fig. 7. Voltage clamp analysis of *Xenopus* oocytes injected with *in vitro*-synthesized GluClα2 RNA. (**A**) A rapidly desensitizing current occurs in response to glutamate in the range from 200 µM to 5 mM. Bars indicate the period of time during which the drug was applied. Below is the concentration–response curve with the normalized maximal response on the Y-axis and glutamate concentration on a log scale on the *x*-axis. The curve represents the average of five oocytes; error bars indicate 1 SEM. Oocytes were clamped at –80 mV unless otherwise indicated. (**B**) An oocyte treated with 10 mM glutamate and subsequently with 10 µM ivermectin. The arrow indicates when ivermectin was applied (exposure to ivermectin was continuous from this point on) and the bar indicates when glutamate was applied. Note that this oocyte was injected with ~20-fold less RNA than the oocytes in (A). (**C**) An *I–V* curve for a GluClα2A-expressing oocyte after treatment with 10 µM ivermectin. ●, *I–V* curve in Ringers (108 mM Cl) as the external solution; ○, *I–V* curve in gluconate–Ringers (8 mM Cl).

remove a potential phosphorylation site in the intracellular domain (Malosio *et al.*, 1991; Macdonald and Olsen, 1994). An α2 glycine receptor subunit has two splice variants that differ in an exon coding for part of the extracellular domain (Kuhse *et al.*, 1991). Although GluClα2 has a potential phosphorylation site in the intracellular loop domain that is conserved with GluClα1, there is no evidence that it is affected by alternative splicing. Rather, the GluClα2A splice variant contains a large extracellular domain not found in any known ligand-gated chloride channel subunits. The role of the large extracellular domain in GluClα2A is not clear, but it does not appear to affect gating by glutamate or ivermectin since GluClα2B and GluClα2A respond similarly to these ligands (J.Dent, unpublished observation). It includes a highly acidic domain and is predicted to be substantially α-helical (Chou and Fasman, 1974). Thus, it may interact with other proteins, perhaps as part of a synaptic localization mechanism.

M3s are fast inhibitory glutamatergic neurons

We present the following evidence that M3 is glutamatergic: (i) When applied to the exposed pharynx, glutamate mimics the effect of the M3 neuron and shortens the duration of the muscle contraction during a pump. (ii) *avr-15*, a mutant that lacks M3-generated IPSPs, is also insensitive to iontophoretically applied glutamate. (iii) *avr-15* acts in the pharyngeal muscle, as indicated by the fact that expression under the *myo-2* promoter rescues M3-generated IPSPs. (iv) *avr-15* encodes a protein, GluClα2A, which forms a homomeric glutamate-gated chloride channel. Taken together, these data indicate that the *avr-15*-encoded chloride channel subunit is part of a glutamate-gated channel that is expressed in the pharyngeal muscle and responds to glutamate released by the M3 neurons at neuromuscular synapses. This is the first demonstration of a fast inhibitory glutamatergic synapse in nematodes (Geary *et al.*, 1993).

The inhibitory, hyperpolarizing effects of glutamate have been demonstrated for neurons of crustaceans (Bidaut, 1980; Eisen and Marder, 1982; Marder and Eisen, 1984), insects (Wafford and Sattelle, 1989) and molluscs (Gerschenfeld and Lasansky, 1964; Walker *et al.*, 1971; Cottrell *et al.*, 1972; Oomura *et al.*, 1974) and glutamate has also been shown to have an inhibitory effect on crustacean (Lingle and Marder, 1981) and insect muscle (Cull-Candy, 1976; Delgado *et al.*, 1989). The effects of glutamate are mediated by chloride and/or potassium and both conductances are often blocked by picrotoxin. In contrast, although vertebrates exhibit a slow inhibitory glutamatergic neurotransmission mediated by metabotropic glutamate receptors, fast glutamatergic neuro-

transmission appears to be strictly excitatory and is mediated by a different class of channels (Nakanishi, 1992). The specificity of ivermectin for channels that mediate inhibitory glutamatergic neurotransmission may in part explain why it is tolerated so well by vertebrates.

GluClα2 confers ivermectin sensitivity on C.elegans

Our results demonstrate that a nematocidal activity of ivermectin is a result of the ability of ivermectin to act as an agonist of chloride channels. Ivermectin appears to act as an agonist by increasing the open time of the receptor (Martin and Pennington, 1989; Zufall *et al.*, 1989). Thus, a mutant that is resistant to ivermectin would be expected to contain a mutation that reduces the activity of the ivermectin-sensitive channel, i.e. a loss-of-function mutation. This is consistent with the molecular evidence that *avr-15(ad1051)* is a null allele. Since GluClα2 forms a homomeric channel that responds to ivermectin, it must itself bind ivermectin rather than merely being necessary for the formation of an ivermectin-sensitive channel.

In order for ivermectin to be lethal, the chloride permeability that it generates must inhibit essential cells or organs. Previous results are consistent with the idea that ivermectin exerts its lethality via its ability to starve worms by inhibiting pharyngeal pumping. Ivermectin inhibited pumping in *C.elegans* and other nematodes (Bottjer and Bone, 1985; Avery and Horvitz, 1990; Geary *et al.*, 1993). *C.elegans* eggs that are placed in ivermectin hatch, but the larvae never grow (J.Dent, unpublished observation); they arrest in the first larval stage, which is a phenotype of worms that are unable to feed (Avery and Horvitz, 1987). However, these results do not rule out indirect effects on the pharynx, which is bathed in the pseudocoelomic fluid and is therefore sensitive to humoral effects and the general health of the worm (L.Avery, unpublished observation). The fact that GluClα2 confers ivermectin sensitivity even when its expression is restricted to pharyngeal muscle using the *myo-2* promoter supports the idea that ivermectin directly inhibits pharyngeal pumping which is sufficient to kill the worm by starvation.

One of the mysteries of ivermectin action that our results may help begin to address is why ivermectin is larvicidal but not adulticidal (Dreyer *et al.*, 1995). If the relevant site of action in parasitic nematodes is also the pharynx, then it may be that growing larvae need to ingest food more efficiently that adults, who have already stored up reserves of food and are not growing. A related question is what role the ability of ivermectin to paralyze worms plays in its nematocidal mechanism (Arena *et al.*, 1995). We showed that GluClα2A appears to be expressed in the nervous system, specifically in motor neurons, and ivermectin may therefore interfere with locomotion via its interaction with receptors expressed on neurons. Severe paralysis has surprisingly little effect on the viability of *C.elegans* grown in the laboratory. Whether paralysis is likely substantially to affect the viability of a parasitic nematode and whether it is likely preferentially to affect larvae probably depends on the particulars of that nematode's life-style.

Carl Johnson first showed that ivermectin resistance is synthetic—in other words, there must be mutations in two genes simultaneously for worms to exhibit high-level (>10-fold) resistance (Rand and Johnson, 1995; C.D.Johnson, unpublished observation cited in Anderson, 1995). We have confirmed this observation by isolating ivermectin-resistant worms from an *avr-15* background. The nature of the other ivermectin-resistant genes is presently unclear; one possibility is that some encode other ivermectin-sensitive channel subunits. As mentioned above, there appear to be multiple *C.elegans* genes encoding putative chloride channel subunits in addition to the genes for GluClα1 and α2 (J.Dent, unpublished observation). Interestingly, when exposed pharynxes of *avr-15(ad1051)* worms are treated with ivermectin, they continue pumping, indicating that ivermectin's other target is extrapharyngeal (J.Dent, unpublished observation).

In spite of ivermectin's widespread use, only isolated cases of resistance have been reported in the field (Clark *et al.*, 1995), possibly because parasitic helminths must also acquire multiple mutations to become resistant. A better understanding of ivermectin resistance in *C.elegans* and in parasitic helminths may indicate strategies for the design of other anthelmintic drugs that do not suffer from the development of resistance in treated populations. Our results suggest that targeting drugs to the protein products of multigene families may be useful in preventing resistance.

Materials and methods

Care of C.elegans

Worms were raised using standard techniques (Sulston and Hodgkin, 1988) and fed *Escherichia coli* strain HB101 or DA837 (Davis *et al.*, 1995). The wild-type strain was Bristol strain N2. The following mutant strains were used: DA1051 *avr-15(ad1051) V*, CB1489 *him-8(e1489) IV*, DA1052 *him-8(e1489) IV; avr-15(ad1051) V*, NS378 *avr-15(nr395) V*, MT5813 *+/nT1(let(–) unc(n754sd)); nDf42 V / nT1(V)*, DA1068 *him-8(e1489) IV; avr-15(nr395) V*, DA438 *bli-4(e937) I; rol-6(e187) II; daf-2(e1368ts) vab-7(e1562) III; unc-31(e928) IV; dpy-11(e224) V; lon-2(e678) X*, DA1302 and RC301.

Genetics

avr-15(ad1051) was isolated in an RC301 background by standard ethyl methanesulfonate mutagenesis techniques (Anderson, 1995) using the clonal starvation screen described previously (Avery, 1993a) with the following modification: worms were screened on the *E.coli* strain DA837 to enhance the starvation phenotype and starved mutants underwent a secondary screen in which only mutants with abnormal EPGs were kept. To test for complementation between *ad1051* and *avr-15*, a *him-8(e1489); avr-15(ad1051)* double was constructed (DA1052) and males from this strain were mated to NS378 [*avr-15(nr395)*]. F_1 male progeny were examined by EPG and found to lack M3 IPSPs. Similarly, a *him-8(e1489); avr-15(nr395)* double was constructed (DA1068) and males from this strain and from DA1052 were mated to the *nDf42* strain MT5813. Non-Unc F_1 male progeny from these crosses were scored by EPG and found to lack M3 IPSPs. Ivermectin-resistant strains were isolated by EMS mutagenesis of *avr-15(ad1051)*, growth of 10 separate pools on normal plates, followed by selection of F_2 eggs on plates containing 1% DMSO/~10 ng/ml ivermectin. Only one resistant worm was isolated from each pool. The worms were 2× outcrossed to N2 by mating N2 males to the resistant strain and then mating the male progeny to N2 hermaphrodites. The F_2 eggs from that cross were reselected for ivermectin resistance on plates containing either 10 or 100 ng/ml ivermectin. Mapping was performed by crossing males from the resistant strain into DA438 and selecting the F_2 eggs on 10 or 100 ng/ml ivermectin.

Electrophysiology

Electropharyngeograms (EPGs) were performed as described by Raizen and Avery (1994) in Dent's saline (Avery *et al.*, 1995) in the absence of serotonin. EPGs of exposed pharynxes were performed and analyzed as described by Davis *et al.* (1995). Iontophoresis pipettes were pulled

on a Sutter P87 pipette puller and filled with a solution of 300 mM sodium glutamate, 50 mM carboxyfluorescein, neutralized to pH 7.0 with potassium hydroxide. The iontophoresis pipette was connected to an electrically isolated current source of our own design (schematic available on request). The resistance of the pipette was typically 50–150 MΩ. The carboxyfluorescein allowed us to see the iontophoretic pulse and confirm that the pipette was working properly. A retaining current of 1–10 nA was applied and the pulse current was typically –25 to –45 nA. The tip of the iontophoresis pipette was maneuvered to a point just posterior of the metacorpus at the approximate position of the M3 neurons (Albertson and Thomson, 1976; at more posterior positions, the glutamate was ineffective). The EPG trace of the exposed pharynx was fed into a Labview (National Instruments) virtual instrument (ACCTRIG written by M.W.Davis, available on request) which recorded the trace, detected the E spike of the EPG, and sent a command voltage to the current source. The current source generated the iontophoretic pulse. The glutamate and aspartate results were obtained in a blind trial. Six tubes of iontophoresis solution containing glutamate and six tubes containing aspartate were coded and tested for their effect on pump length. Some negatives (samples that had no effect on the pharynx) had to be re-tested to obtain a total of six positives, indicating that false negatives can occur. We never saw false positives. Since we cannot distinguish lack of effect from a false negative, some of the aspartate data included in the graph may be the result of false negatives. The effect of chloride concentration was tested by dissecting six worms into Dent's saline in which the sodium chloride was replaced with sodium gluconate. The same pharynxes were re-tested after replacing one-half of the buffer with normal Dent's saline. Pumps that extended beyond the 3-s recording window were treated as 3 s long. The data in Figure 2B were collected as part of a blind test comparing *eat-4* with *avr-15* mutants. The blind test was performed by coding six plates of *avr-15(ad1051)* worms and six plates of *eat-4(ad572)* worms. The mutant worms were grown on HB101 bacteria to mask their starvation phenotype (Davis *et al.*, 1995) and appeared indistinguishable from each other. Some negatives were retested until the sixth positive was found. As noted for the aspartate data in Figure 2B, some of the *avr-15* data included in the graph may be the result of false negatives. In all figures, a one-tailed Mann–Whitney *U*-test was used to determine statistical significance of the difference between the (–) and (+) bars in each category.

Laser ablation

The M3 neurons of six wild type worms were killed by ablating the neurons with a laser using the protocol described in Raizen and Avery (1994; see also Bargmann and Avery, 1995). A sampling of the laser kills were verified by noting the absence of M3 activity in the EPG of operated worms.

Molecular biology

All molecular biology was performed according to standard methods as described in Sambrook *et al.* (1989). All plasmid subcloning was into pBluescript KS(+) (Stratagene, La Jolla, CA). A 2.2 kb GluClα1 genomic fragment was generated by PCR of DNA from wild-type worms using the primers GCTTCCGGTACCCCTCAATACTGCATAAATTGGC and CCATGGGAGCTCTAAAATAATACGTTCTGCTGGCC and was subcloned. The identity of this clone was confirmed by partial sequencing using the PCR primers. The GluClα1 fragment was used to probe a *C.elegans* YAC grid. A weakly hybridizing signal to the overlapping YACs Y53F11, Y55E8 and Y47E2 identified K10B8 as a cosmid likely to contain DNA encoding the hybridizing sequence. Southern blots of a restriction digest of K10B8 identified a 4 kb *Bam*HI–*Hin*dIII fragment that hybridized to GluClα1. The *Bam*HI–*Hin*dIII fragment was subcloned and both strands sequenced with Sequenase Version 2.0 (United States Biochemicals, Cleveland, OH) on deletions generated by the *Exo*III/S1 method (Henikoff, 1987). Customized sequencing primers were used to fill in the gaps. The GluClα1 clone was used to probe 480 000 plaques from a mixed-stage *C.elegans* cDNA library (Stratagene, La Jolla, CA). The primary and secondary plaques were reprobed with a ~1 kb *Xba*I–*Bam*HI K10B8 fragment using the T7 and T3 pBluescript primers to generate a PCR probe. The excised cDNAs in pBluescript SK^- were generated by co-transfection of the isolated plaques with helper phage. The longest cDNA, gluA1, was *Exo*III/S1 deleted and sequenced on one strand. We generated a probe corresponding to the ~600 bp at the 5′ end of gluA1 by PCR using the T3 primer and the primer CTGTGTCAGATGTTTGAGGT. When used to probe restriction digests of K10B8, the 5′ gluA1 probe hybridized to a ~1.5 kb *Xho*I–*Pst*I fragment and an adjoining ~6 kb *Pst*I–*Sac*I fragment on Southern blots. These fragments were subcloned, *Exo*III/S1 deleted and partially sequenced on both strands by ABI DNA sequencer using dye terminator reactions.

RNA was isolated from N2 and DA1051 worms using RNA Stat-60 (Tel-Test B, Friendswood, TX) and poly(A)$^+$ selected using oligo(dT) columns (5′-3′, Boulder, CO). The RNA was run on a formaldehyde gel and blotted. A double-stranded probe was generated by PCR of gluA1 cDNA using CCCCATATGATAGGTCGATTGCGGAGAGGCT ('oo-5') and AAGGTGCTCCAGAATTTCTGT ('cds-3'). The bands were quantitated using a Molecular Dynamics (Sunnyvale, CA) model 300 densitometer and ImageQuant software. A *t*-test was used to calculate the minimum intensity ratio of Northern bands over background. The ratio of the 2.2 kb band to the 1.7 kb band was calculated based on the intensity of the two bands on the Northern, normalizing for the actin loading controls. 5′ RACE was performed to identify the 5′ ends of the two transcripts using the 5′ RACE kit (Gibco-BRL, Gaithersburg, MD). 100 ng poly(A)$^+$ RNA was reverse transcribed using the 'cds-3' primer. We identified the 5′ end of the 1.7 kb transcript by amplifying the cDNA with a primer corresponding to the SL-1 trans-spliced leader sequence ('SL1-Bam'; Krause, 1995) and GCTCTAGAGTTGTTCAATTGGTACATGT, cloning into *Bam*HI and *Xba*I sites of Bluescript KS+ and sequencing. The 5′ end of the larger transcript was identified by dC tailing the cDNA and amplifying with an anchored primer and GTTGATGTTGCGGGTTCAACT. The PCR product was diluted and amplified with the 'universal amplification' primer and CAUCAUCAUCAUGGAACAAGATGAAGCCTCT where U is deoxyuridine. The product was cloned using the pAMP system (Gibco-BRL) and sequenced.

Identification of the ad1051 mutation

To identify the mutation in *avr-15(ad1051)*, exons were amplified by PCR with the following primers which hybridize to intron sequences: exon 1, GGGGTACCGCTCTTCCATAGCTCTTTGGGAGT and GGGGTACCGTGTTAGTCGAGATATCCGACT; exon 2, GGGGTACCCTGGGATACGATGAGAGCAGA and GGGGTACCGGGCCTTTGGGATGTT-AAGTT; exon 3, GGGGTACCCTCGCGGAACACGTGTCACGT and GGGGTACCTGAAGAGGTCCCTTCTTATGAA; exon 4, GGGGTACCTTAAGAGTAGCTGTTAGCCGA and GGGGTACCGATGGAATTAGGGGATCTCCTGA; exon 5, CGCGGATCCAGTGGAATTTAAATGCGCGATAGT and CGCGGATCCTGACTACAAGCAATGTTAGA; exon 6, CGCGGATCCAGGACTAAAATGAAGGTTCCCA and CGCGAATCCTCTCTCTTTCAGTTCGA; exon 7, CGCGGATCCTGTCAAGTTTGATATCATCTCA and CGCGGATCCGCAAGATGCTAATAAGAGTCA. The PCR products were digested with either *Kpn*I (exons 1–4) or *Bam*HI (exons 5–7) and cloned into the *Kpn*I and *Bam*HI sites of pBluescript KS+ respectively. Three independent PCR clones for each exon were sequenced by ABI sequencer with either T7 or M13 reverse primers and dye terminator reactions.

myo-2::GluClα2A and pT7NGluClα2A and avr-15::GFP constructs

The A1 cDNA was PCR amplified using the primers 'oo-5' and CCCTCTAGACGTACTGATGGCCACACCGT and TA cloned into pCR II (Invitrogen Corp., San Diego, CA). The insert was re-cloned into pBluescript KS(+) using the *Bam*HI and *Xba*I sites. To create *myo-2*::GluClα2A, the 3′ end of the PCR product was fused, at the *Xho*I site, to genomic DNA encoding some open reading frame and the 3′-UTR of *avr-15*. The insert was cut out with *Spe*I and *Sac*I and cloned into the *Nhe*I and *Sac*I sites of pPD30.69 [all pPD vectors courtesy of A.Fire, J.Ahn, G.Seydoux and S.Xu (Mello and Fire, 1995)]. To create pT7NGluClα2A, the insert was cloned into pT7N, a modified pSP64T transcription vector (Cary *et al.*, 1994) using the *Nde*I and *Xba*I sites. To create the GFP promoter fusion, a synthetic transmembrane domain from pPD34.110 (Fire *et al.*, 1990) was cloned in place of the nuclear localization signal in pPD95.73. The transmembrane domain fused to GFP was removed using *Pst*I and *Apa*I and cloned in-frame to a 6 kb (*Sac*I–*Pst*I) genomic fragment at the *Pst*I site in the open reading frame and the *Apa*I site in vector. Pictures (Figures 4 and 6) were annotated and contrast-enhanced using Adobe Photoshop 3.0 (Mountain View, CA).

Oocyte expression

RNA was transcribed from pT7NGluClα2A using T7 polymerase and ~50 nl of RNA (~1 μg/μl) dissolved in water was injected into each oocyte. Oocytes were incubated 2–6 days at 16°C until experiments were performed at room temperature. Two-electrode voltage clamp was performed using an Axoclamp 2B (Axon Instruments, Foster City, CA). Oocytes were in Ringers solution (100 mM NaCl, 1.8 mM KCl, 2 mM $CaCl_2$, 1 mM $MgCl_2$, 5 mM HEPES, pH 7.8) or Ringers/1% DMSO for

solutions containing ivermectin. Recording electrodes were filled with 3 M KCl and the bath electrode was connected via a 3 M KCl agar bridge. Solutions of glutamate or ivermectin in Ringers were applied to oocytes in a Warner Instruments (Hamden, CT) RC-24 perfusion chamber. Data were acquired and analyzed as described under Electrophysiology; some data were analyzed with Axograph software (Axon Instruments). To generate the concentration–response curve, curves from five different oocytes were fitted to the equation:

$$I_{max} = 1/[1 + (EC_{50}/[D])^h]$$

where I_{max} is the maximal response, [D] is the concentration of glutamate, EC_{50} is the glutamate concentration producing a half-maximal effect, and h is the Hill coefficient. I_{max}, EC_{50} and h were free parameters. The curves were then normalized to the estimated I_{max}. The EC_{50} from the five separate curves were averaged to generate the estimate of the EC_{50} with SEM (see Results). To generate *I–V* curves, current generated by a 3-s voltage clamp from –80 to +30 mV before drug application was subtracted from the current resulting from a post-application voltage clamp. For chloride substitution, the bath Ringers was replaced by Ringers made with Na gluconate instead of NaCl (final chloride concentration 7.8 mM).

Transformation

K10B8 and *myo-2*::gluA1cDNA at a concentration of 1 μg/ml were microinjected into the syncytial gonads of adult hermaphrodites according to standard procedures (Mello and Fire, 1995). The co-transfection marker *rol-6* contained on the pRAK3 plasmid (Davis *et al.*, 1995) was co-injected at a concentration of 70 μg/ml and transformants were identified by the roller phenotype.

Ivermectin sensitivity assay

NGMSR plates (Avery, 1993a) containing 1% DMSO and various concentrations of ivermectin were poured and spotted with *E.coli* strain HB101. Eggs were isolated from gravid adult hermaphrodites by the alkaline bleach method (Lewis and Fleming, 1995), resuspended in M9 buffer, and ~100 eggs were placed on the bacterial lawn of the ivermectin-containing plates. The number of worms reaching adulthood, as determined by the presence of eggs in the uterus, was counted periodically for 2 weeks. If the strain was resistant to ivermectin, then >50 worms grew to adulthood. If the strain was sensitive, then all worms were arrested as larvae. Approximately 200 eggs from the *avr(ad1302); avr-15(ad1051); Ex[myo-2*::gluA1cDNA] strain were placed on each plate and the number of adult rollers was counted after 4 days.

Acknowledgements

We wish to thank Carl Johnson for providing ivermectin-resistant mutants. We are grateful to George Hess for allowing L.A. to perform caged glutamate experiments in his lab, the results of which inspired this work. We thank Jim Hudspeth, Carl Johnson, Raymond Lee, David Raizen, Dean Smith and Steve Wasserman for helpful comments on the manuscript. We thank Linda Doolittle and Shirley Hall for help with sequencing and Raymond Lee for help with library screening. This work was supported by a fellowship from the Klingenstein Foundation to L.A. J.A.D. was supported by a post-doctoral fellowship from the American Cancer Society; M.W.D. was supported by a predoctoral fellowship from the National Science Foundation.

References

Albertson,D.G. and Thomson,J.N. (1976) The pharynx of *Caenorhabditis elegans*. *Philos. Trans. R. Soc. Lond. B*, **275**, 299–325.

Anderson,P. (1995) Mutagenesis. In Epstein,H.F. and Shakes,D.C. (eds), *C. elegans: Modern Biological Analysis of an Organism.* Academic Press, New York, pp. 31–54.

Arena,J.P., Liu,K.K., Paress,P.S., Frazier,E.G., Cully,D.F., Mrozik,H. and Schaeffer,J.M. (1995) The mechanism of action of avermectins in *Caenorhabditis elegans*: correlation between activation of glutamate-sensitive chloride current, membrane binding and biological activity. *J. Parasitol*., **81**, 286–294.

Avery,L. (1993a) The genetics of feeding in *C. elegans*. *Genetics*, **133**, 897–917.

Avery,L. (1993b) The motor neuron M3 controls pharyngeal muscle relaxation timing in *Caenorhabditis elegans*. *J. Exp. Biol*., **175**, 283–297.

Avery,L. and Horvitz,H.R. (1987) A cell that dies during wild type *C. elegans* development can function as a neuron in a ced-3 mutant. *Cell*, **51**, 1071–1078.

Avery,L. and Horvitz,H.R. (1990) The effects of starvation and neuroactive drugs on feeding in *Caenorhabditis elegans*. *J. Exp. Zool*., **253**, 263–270.

Avery,L., Lockery,S. and Raizen,D.M. (1995) Electrophysiological methods. In Epstein,H.F. and Shakes,D.C. (eds), *C. elegans: Modern Biological Analysis of an Organism*. Academic Press, New York, pp. 251–261.

Bargmann,C.I. and Avery,L. (1995) Laser killing of cells in *C. elegans*. In Epstein,H.F. and Shakes,D.C. (eds), *C. elegans: Modern Biological Analysis of an Organism*. Academic Press, New York, pp. 225–250.

Bechade,C., Sur,C. and Triller,A. (1994) The inhibitory neuronal glycine receptor. *BioEssays*, **16**, 735–744.

Bidaut,M. (1980) Pharmacological dissection of pyloric network of the lobster stomatogastric ganglion using picrotoxin. *J. Neurophysiol*., **44**,1089–1101.

Bottjer,K.P. and Bone,L.W. (1985) *Trichostrongylus colubriformis*: effect of anthelmintics on ingestion and oviposition. *Int. J. Parasitol*., **15**, 501–503.

Campbell,W.C. (1989) *Ivermectin and Abamectin*. Springer-Verlag, New York.

Cary,R.B., Klymkowsky,M.W., Evans,R.M., Domingo,A., Dent,J.A. and Backhus,L.E. (1994) Vimentin's tail interacts with actin-containing structures *in vivo*. *J. Cell Sci*., **107**, 1609–1622.

Chang,Y., Wang,R., Barot,S. and Weiss,D.S. (1996) Stoichiometry of a recombinant $GABA_A$ receptor. *J. Neurosci*., **16**, 5415–5424.

Chou,P.Y. and Fasman,G.D. (1974) Prediction of protein conformation. *Biochemistry*, **13**, 222–245.

Clark,J.M., Scott,J.G. and Campos,F. (1995) Resistance to avermectins: extent mechanisms and, management implications. *Annu. Rev. Entomol*., **40**, 1–30.

Cottrell,G.A., Macon,J. and Szczepaniak,A. (1972) Glutamic acid mimicking of synaptic inhibition on the giant serotonin neurone on the snail. *Br. J. Pharmacol*., **45**, 684–687.

Cull-Candy,S.G. (1976) Two types of extrajunctional L-glutamate receptors in locust muscle fibres. *J. Physiol. Lond*., **255**, 449–464.

Cully,D.F., Vassilatis,D.K., Liu,K.K., Paress,P.S., Van der Ploeg,L.H.T., Schaeffer,J.M. and Arena,J.P. (1994) Cloning of an avermectin-sensitive glutamate-gated chloride channel from *Caenorhabditis elegans*. *Nature*, **371**, 707–711.

Cully,D.F., Paress,P.S., Liu,K.K., Schaeffer,J.M. and Arena,J.P. (1996) Identification of a *Drosophila melanogaster* glutamate-gated chloride channel sensitive to the antiparasitic agent avermectin. *J. Biol. Chem*., **271**, 20187–20191.

Davis,M.W., Somerville,D., Lee,R.Y.N., Lockery,S., Avery,L. and Fambrough,D.M. (1995) Mutations in the *Caenorhabditis elegans* Na,K-ATPase α-subunit gene, *eat-6*, disrupt excitable cell function. *J. Neurosci*., **15**, 8408–8418.

Delgado,R., Barla,R., Latorre,R. and Labarca,P. (1989) L-glutamate activates excitatory and inhibitory channels in *Drosophila* larval muscle. *FEBS Lett*., **243**, 337–342.

Dreyer,G., Noroes,J., Amaral,F., Nen,A., Medeiros,Z., Coutinho,A. and Addiss,D. (1995) Direct assessment of the adulticidal efficacy of a single dose of ivermectin in bancroftian filariasis. *Trans. R. Soc. Trop. Med. Hyg*., **89**, 441–443.

Duce,I.R. and Scott,R.H. (1985) Actions of dihydroavermectin B1a on insect muscle. *Br. J. Pharmacol*., **85**, 395–401.

Eisen,J.S. and Marder,E. (1982) Mechanisms underlying pattern generation in lobster stomatogastric ganglion as determined by selective inactivation of identified neurons. III. Synaptic connections of electrically coupled pyloric neurons. *J. Neurophysiol*., **48**, 1392–1415.

Etter,A., Cully,D.F., Schaeffer,J.M., Liu,K.K. and Arena,J.P. (1996) An amino acid substitution in the pore region of a glutamate-gated chloride channel enables the coupling of ligand binding to channel gating. *J. Biol. Chem*., **271**, 16035–16039.

Fire,A., White-Harrison,S. and Dixon,D. (1990) A modular set of *lacZ* fusion vectors for studying gene expression in *Caenorhabditis elegans. Gene*, **93**, 189–198.

Fritz,L.C., Wang,C.C. and Gorio,A. (1979) Avermectin B1a irreversibly blocks postsynaptic potentials at the lobster neuromuscular junction by reducing muscle membrane resistance. *Proc. Natl Acad. Sci. USA*, **76**, 2062–2066.

Geary,T.G., Klein,R.D., Vanover,L., Bowman,J.W. and Thompson,D.P. (1992) The nervous system of helminths as targets for drugs. *J. Parasitol*., **78**, 215–230.

Geary,T.G., Sims,S.M., Thomas,E.M., Vanover,L., Davis,J.P., Winterrowd,C.A., Klein,R.D., Ho,N.F.H. and Thompson,D.P. (1993) Haemonchus contortus: ivermectin-induced paralysis of the pharynx. *Exp. Parasitol*., **77**, 88–96.

Gerschenfeld,H.M. and Lasansky,A. (1964) Action of glutamic acid and other naturally occurring amino-acids on snail central neurons. *Int. J. Neuropharmacol*., **3**, 301–314.

Grenningloh,G., Pribilla,I., Prior,P., Multhaup,G., Beyreuther,K., Taleb,O. and Betz,H. (1990) Cloning and expression of the 58 kDa β subunit of the inhibitory glycine receptor. *Neuron*, **4**, 963–970.

Henikoff,S. (1987) Unidirectional digestion with exonuclease III in DNA sequence analysis. *Methods Enzymol*., **155**, 156–165.

Krause,M. (1995) Transcription and translation. In Epstein,H.F. and Shakes,D.C. (eds), *C. elegans: Modern Biological Analysis of an Organism*. Academic Press, New York, pp. 31–54.

Kuhse,J., Kurytov,A., Maulet,Y., Malosio,M.-L., Schmeiden,V. and Betz,H. (1991) Alternative splicing generates two isoforms of the α2 subunit of the inhibitory glycine receptor. *FEBS Lett*., **283**, 73–77.

Kusano,K., Miledi,R. and Stinnakre,J. (1982) Cholinergic and catecholaminergic receptors in the *Xenopus* oocyte membrane. *J. Physiol*., **328**, 143–170.

Laughton,D.L., Wolstenholme,A.J. and Lunt,G.G. (1995) The beta subunit of the *C. elegans* inhibitory glutamate receptor is expressed on the pm4 pharyngeal muscle cells. Abstract 167.9, *J. Neurosci. Abs*., **21**, 406.

Lees,G. and Beadle,D.J. (1986) Dihydroavermectin B1: actions on cultured neurones from the insect central nervous system. *Brain Res*., **366**, 369–372.

Lewis,J.A. and Fleming,J.T. (1995) Basic culture methods. In Epstein,H.F. and Shakes,D.C. (eds), *C. elegans: Modern Biological Analysis of an Organism*. Academic Press, New York, pp. 12–14.

Lingle,C. and Marder,E. (1981) A glutamate-activated chloride conductance on crustacean muscle. *Brain Res*., **212**, 481–488.

Liu,L.X. and Weller,P.F. (1996) Antiparasitic drugs. *N. Engl. J. Med*., **334**, 1178–1184.

Macdonald,R.L. and Olsen,R.W. (1994) $GABA_A$ receptor channels. *Annu. Rev. Neurosci*., **17**, 569–602.

Malosio,M.-L., Grenningloh,G., Kuhse,J., Scheiden,V., Schmitt,B., Prior,P. and Betz,H. (1991) Alternative splicing generates two variants of the α1 subunit of the inhibitory glycine receptor. *J. Biol. Chem*., **266**, 2048–2053.

Marder,E. and Eisen,J.S. (1984) Transmitter identification of pyloric neurons: electrically coupled neurons use different transmitters. *J. Neurophysiol*., **51**, 1345–1361.

Martin,R.J. (1993) Neuromuscular transmission in nematode parasites and antinematodal drug action. *Pharmacol. Ther*., **58**, 13–50.

Martin,R.J. and Pennington,A.J. (1989) A patch–clamp study of effects of dihydroavermectin on *Ascaris* muscle. *Br. J. Pharmacol*., **98**, 747–756.

McIntire,S.L., Jorgensen,E. and Horvitz,H.R. (1993a) Genes required for GABA function in *Caenorhabditis elegans*. *Nature*, **364**, 334–337.

McIntire,S.L., Jorgensen,E., Kaplan,J. and Horvitz,H.R. (1993b) The GABAergic nervous system of *Caenorhabditis elegans*. *Nature*, **364**, 337–341.

Mellin,T.N., Busch,R.D. and Wang,C.C. (1983) Postsynaptic inhibition of invertebrate neuromuscular transmission by avermectin B1a. *Neuropharmacology*, **22**, 89–96.

Mello,C., and Fire,A. (1995) DNA Transformation. In Epstein,H.F. and Shakes,D.C. (eds), *Caenorhabditis elegans: Modern Biological Analysis of an Organism*. Academic Press, NY, pp. 452–482.

Nakanishi,S. (1992) Molecular diversity of glutamate receptors and implications for brain function. *Science*, **258**, 597–603.

Okkema,P.G., Harrison,S.W., Plunger,V., Aryana,A. and Fire,A. (1993) Sequence requirements for myosin gene expression and regulation in *Caenorhabditis elegans*. *Genetics*, **135**, 385–404.

Oomura,Y., Ooyama,H. and Sawada,M. (1974) Analysis of hyperpolarizations induced by glutamate and acetylcholine on onchidium neurones. *J. Physiol. Lond*., **243**, 321–341.

Pong,S.-S. and Wang,C.C. (1982) Avermectin B1a modulation of γ-aminobutyric acid receptors in rat brain. *J. Neurochem*., **38**, 375–379.

Pulak,R. and Anderson,P. (1993) Messenger RNA surveillance by the *Caenorhabditis elegans smg* genes. *Genes Dev*., **7**, 1885–1897.

Raizen,D.M. and Avery,L. (1994) Electrical activity and behavior in the pharynx of *Caenorhabditis elegans*. *Neuron*, **12**, 483–495.

Rand,J.B. and Johnson,C.D. (1995) Genetic pharmacology. In Epstein,H.F. and Shakes,D.C. (eds), *C. elegans: Modern Biological Analysis of an Organism*. Academic Press, New York, pp. 187–201.

Sambrook,J., Fritsch,E.F. and Maniatis,T. (1989) *Molecular Cloning: A Laboratory Manual*. 2nd edn. Cold Spring Harbor Laboratory Press, Cold Spring Harbor, NY.

Sigel,E. and Baur,R. (1987) Effect of avermectin B1a on chick neuronal γ-aminobutyrate receptor channels expressed in *Xenopus* oocytes. *Mol. Pharmacol*., **32**, 749–752.

Sulston,J.E. and Hodgkin,J.G. (1988). Methods. In Wood,W. (ed.), *The Nematode Caenorhabditis elegans*. Cold Spring Harbor Laboratory Press, Cold Spring Harbor, NY, pp. 587–606.

Thompson,J.D., Higgins,D.G. and Gibson,T.J. (1994) CLUSTAL W: improving the sensitivity of progressive multiple sequence alignment through sequence weighting, position specific gap penalties and weight matrix choice. *Nucleic Acids Res*., **22**, 4673–4680.

von Heijne,G. (1986) A new method for predicting signal sequence cleavage sites. *Nucleic Acids Res*., **14**, 4683–4690.

Wafford,K.A. and Sattelle,D.B. (1989) L-glutamate receptors on the cell body membrane of an identified insect motor neurone. *J. Exp. Biol*., **144**, 449–462.

Walker,R.J., Woodruff,G.N. and Kerkut,G.A. (1971) The effect of ibotenic acid and muscimol on single neurons of the snail, *Helix aspersa*. *Comp. Gen. Pharmacol*., **2**, 168–174.

Zufall,F., Franke,C. and Hatt,H. (1989) The insecticide avermectin B1a activates a chloride channel in crayfish muscle membrane. *J. Exp. Biol*., **142**, 191–205.

Received on February 7, 1997; revised on July 3, 1997

Note added in proof

'H.Li, W.Denk, L.Avery and G.Hess, unpublished observation' has been published [Li,H., Avery,L., Denk,W. and Hess,G.P. (1997) Identification of chemical synapses in the pharynx of *Caenorhabditis elegans. Proc. Natl Acad. Sci. USA*, **94**, 5912–5916.] The DDBJ/EMBL/GenBank accession Nos. for GluCLα2A and GluClαB are AJ000538 and AJ000537 respectively. M.W.D. was supported by National Institutes of Health training grant 5T32GM08203.